

BROADBAND SINGLE-FED SINGLE-PATCH CIRCULARLY POLARIZED MICROSTRIP ANTENNA

F. Xu*, X.-S. Ren, Y.-Z. Yin, and S.-T. Fan

National Key Laboratory of Science and Technology on Antennas and Microwaves, Xidian University, Xi'an, Shaanxi 710071, China

Abstract—The paper demonstrates a novel antenna which can achieve a broad impedance bandwidth and circularly polarized bandwidth with a suspended corner-truncated square patch and a new probe-fed rectangular strip. By incorporating a probe-fed rectangular strip inside a high substantial cavity ($\sim 0.144\lambda_0$), a broad impedance bandwidth (VSWR < 2.0) of 770 MHz (31.43%) is achieved. To obtain a good circularly polarized (CP) bandwidth matching with the impedance bandwidth, two stubs with optimized lengths are loaded at the non-radiating edges of the corner-truncated square patch symmetrically. Measured results show that the CP antenna features a wide operating bandwidth of 10% ranging from 2.41 GHz to 2.66 GHz (VSWR < 1.5 and axial ratio < 3 dB) and that of 22.45% ranging from 2.31 GHz to 2.86 GHz (VSWR < 2 and axial ratio < 6 dB) and good radiation patterns with cross-polarization level (LHCP) lower than the co-polarization level (RHCP) by more than 20 dB at the broadside direction. The average gain of this antenna is recorded as about 8.16 dBi across the operating bandwidth.

1. INTRODUCTION

In the past decades, microstrip patch antenna technique has been developed rapidly [1–6]. However, the design of a broadband circularly polarized patch antenna that uses a single feed has long been a challenging problem, as compared to the design of linearly polarized (LP) and the dual-fed circularly polarized (CP) patch antennas [7, 8]. Especially, the single-fed single-patch CP antenna has inherently narrow impedance and axial ratio (AR) bandwidths of 1%–2% [9, 10].

Received 16 September 2012, Accepted 12 November 2012, Scheduled 14 November 2012

* Corresponding author: Feng Xu (624550103@qq.com).

In order to achieve enhanced CP bandwidth, several single-fed single-element patch antenna designs using an air-layer or foam substrate have also been shown [11–13], in which the reported CP bandwidths are about 3.5% [11,12] and 7.2% [13]. Besides that, the U-slot and L-probe techniques have been applied to single-layer single-feed circularly polarized antennas [14–17]. These techniques enable the use of thick substrates, and yield axial-ratio bandwidths as large as 13%. Apart from these techniques, the technique of an E-shaped patch used for a broad impedance bandwidth is modified to generate circularly polarized radiation in [18], which uses a single-layer probe-fed patch antenna with a relatively wideband axial ratio (9% for 3 dB AR), without the necessity of it being square or comer-trimmed. Moreover, a wideband H-shaped patch antenna for circular polarization is described in [19], which adapts a printed monopole that is diagonally coupled to the H-shaped copper plate and obtains a wide operational bandwidth of 19.4%. These researches give us some effective methods to achieve wideband CP antenna. Thereinto, since a metal plate directly suspended over a ground plane at a large fractional height of the free-space wavelength, which not only just minimizes the fabrication cost but also eradicates the dielectric loss, thus suspended plate/patch antenna (SPA) has become one of the simple yet cost-effective approaches to improve the bandwidth [20].

In [21], a novel single-fed single-patch broadband circularly polarized antenna is proposed for radio frequency identification (RFID) reader, which reports that a thicker substrate (about $0.12\lambda_0$) is used to enhance the axial ratio bandwidth considerably and a new probe-fed meandered strip feed technique is proposed to tune the impedance matching frequency band to overlap the 3 dB axial ratio frequency band. But the relative 3 dB AR bandwidth of 7.9% makes more room to be broadened further. Moreover, the probe-fed meandered strip is not easy to tune in practice. Based on that antenna model, the proposed design gives a novel antenna structure using a rectangular strip instead of the meandered one, which not only simplifies the antenna structure, but also can obtain a better performance with an impedance bandwidth ($VSWR < 2.0$) of 770 MHz (31.43%), a 3 dB AR bandwidth of 250 MHz (10%) and a 6 dB AR bandwidth of 560 MHz (22.45%).

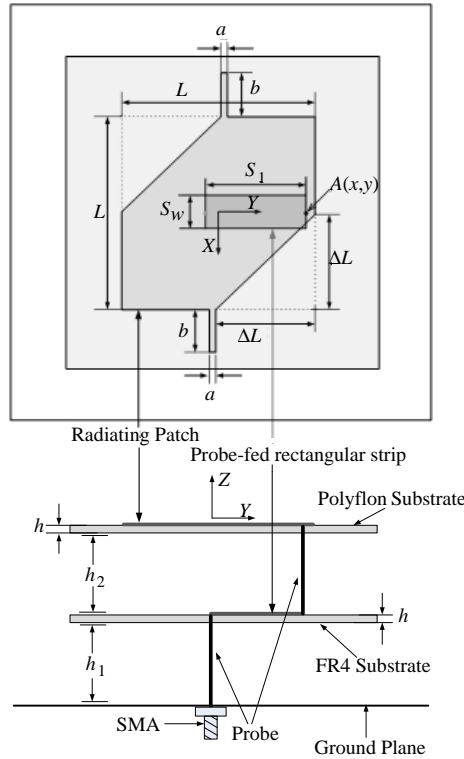
As is known, the art of the CP antenna design is to tailor the mean frequency of its axial-ratio (AR) bandwidth close to that of the impedance bandwidth so that a wide overlapped/operational bandwidth of the CP antenna can be attained [19]. This paper gives us a novel method to align the impedance and AR bandwidths together, without complex systematic tuning. Concretely, two stubs

with optimized lengths are involved to be loaded at the radiating patch of the antenna as shown in Figure 1, which is exclusively to adjust the impedance and axial-ratio bandwidths together. Obviously, this method simplifies the design of the CP antenna further.

2. DESCRIPTION OF ANTENNA AND DESIGN

The geometry of the single-fed single-patch broadband CP microstrip antenna is shown in Figure 1. The center frequency of the antenna is chosen at $f_0 = 2.45$ GHz ($\lambda_0 = 122.4$ mm). As is well known, when a square patch is truncated at corners to generate adequate two orthogonal modes, the antenna radiates CP wave. Based on this theory, the radiating patch is designed to be a square patch with a dimension of $38 \text{ mm} \times 38 \text{ mm}$ ($\sim 0.31\lambda_0 \times 0.31\lambda_0$) and the truncation ΔL of 19 mm. The aluminum plate of the dimensions $117 \text{ mm} \times 137 \text{ mm} \times 2 \text{ mm}$ ($\sim 0.96\lambda_0 \times 1.12\lambda_0 \times 0.016\lambda_0$) is used to approximate the infinite ground plane. A narrow copper rectangular strip of dimensions $20 \text{ mm} \times 10 \text{ mm}$ is horizontally placed between the radiating patch and the ground plane. The radiating patch and the rectangular strip are printed on the upper side of the Polyflon substrate ($\varepsilon_r = 2.55$) and the FR4 substrate ($\varepsilon_r = 4.4$), respectively. One end of the rectangular strip is connected to the radiating patch by the probe of the diameter of $d = 1.2$ mm, while the other end is connected to an SMA probe. The FR4 substrate with a dimension of $60 \text{ mm} \times 60 \text{ mm}$ is suspended above the ground plane at a height of $h_1 = 8$ mm, and the Polyflon substrate with a dimension of $60 \text{ mm} \times 60 \text{ mm}$ is suspended above the rectangular strip at spacing of $h_2 = 8$ mm. Also note that the FR4 substrate and the Polyflon substrate have the same thickness $h = 0.8$ mm. The feed point A (0 mm, 17 mm) is the center point of the projective circle of the probe connected to the radiating patch on the X - Y coordinate plane.

By properly selecting S_l (the length of the rectangular strip, 20 mm) and S_w (the width of the rectangular strip, 10 mm), the input reactance and resistance can be controlled to achieve good impedance matching. Besides that, the large inductance introduced by the long probes in the thick air-layer substrate can be compensated by the electromagnetic coupling between the radiating patch and the probe-fed rectangular strip. In general, this simple but effective technique to broaden the impedance bandwidth is a little bit similar to that of the design with the probe-fed half-wavelength strip [22]. Both of them can be seen as impedance matching networks. However, the length of the probe-fed rectangular strip is just about $0.16\lambda_0$, not the half wavelength.



Parameters	L	ΔL	S_1	S_w	a	b	$h_1=h_2$	h	d
Value/mm	38 ($0.31\lambda_0$)	19 ($0.155\lambda_0$)	20 ($0.163\lambda_0$)	10 ($0.082\lambda_0$)	2 ($0.016\lambda_0$)	8.5 ($0.069\lambda_0$)	8 ($0.065\lambda_0$)	0.8 ($0.007\lambda_0$)	1.2 ($0.01\lambda_0$)

Figure 1. The geometry of the proposed broadband CP microstrip antenna.

3. RESULTS AND DISCUSSION

To investigate the performance of the proposed antenna, the commercial EM software HFSS 13 is used for simulation and optimization. And the optimized dimensions of a fabricated antenna are shown in Figure 1. Two photographs of the broadband CP antenna prototype are shown in Figure 2. It can be seen that the suspended radiating patch, the rectangular strip, two probes and the ground plane are mounted together by means of four long nylon bolts. The

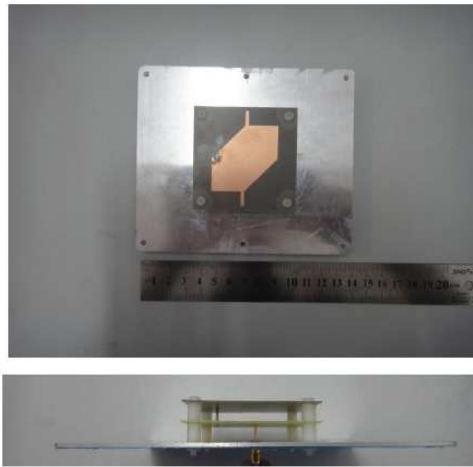


Figure 2. Photographs of the proposed antenna.

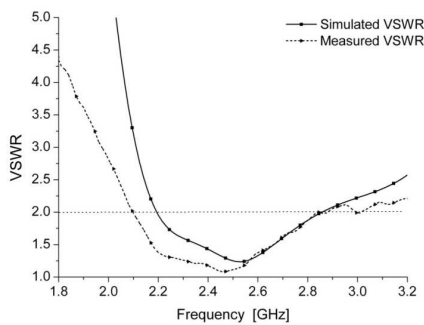


Figure 3. Simulated and measured antenna VSWR.

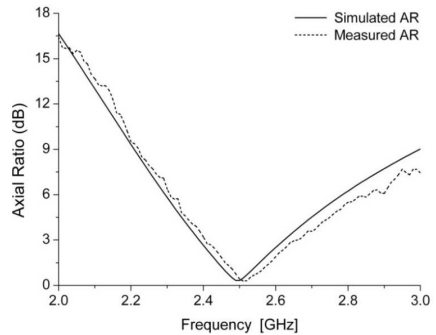


Figure 4. Simulated and measured antenna 3 dB axial-ratios.

simulated and measured VSWR and bore sight axial-ratios for the proposed antenna are shown in Figure 3 and Figure 4, respectively.

As can be seen in Figure 3, an impedance bandwidth (VSWR < 2) of 2.2~2.845 GHz (26.33%) has been obtained in simulation and that of 2.105~2.875 GHz (31.43%) has been measured through a vector network analyzer, Agilent E8357A. The measured impedance bandwidth is basically corresponded with the simulated results. The discrepancy of the measured and simulated results is mainly due to two factors including the variation of the characteristic parameters of the selected medium material and the power loss led by fabrication

such as the existed soldering tins. When fabricated in practice, the dielectric constant ϵ and the dielectric loss tangent $\tan \delta$ of the selected medium materials will have some discrepancy with the theoretical value in simulation. In case the real dielectric constant ϵ becomes less than the theoretical value, the measured impedance bandwidth will be effectively widen. Besides that, larger is the dielectric loss tangent $\tan \delta$, more power loss exists in the practical antenna. All of the power loss makes more power fed through the SMA port be absorbed and the reflected power be reduced. Consequently, the parameter of S_{11} will be lower and the measured impedance bandwidth can be broaden further.

From Figure 4, the proposed CP antenna has a wide 3 dB axial-ratio bandwidth of 2.39~2.62 GHz (9.4%) in simulation and that of 2.41~2.66 GHz (10%) from the measurement. And the measured lowest value of AR is recorded as 0.293 dB, which approaches 0 dB. Although it shifts to high frequency slightly, the measured 3 dB axial-ratio curve is well corresponded with the theoretical simulated result. This frequency-shift is due to measurement error and the fabrication tolerances such as the error of practical dimension of the two subs. And the length of the two subs can affect the resonant frequency of the AR sensitively as shown in Figure 6.

These wideband characteristics above are mainly attributed to two factors: the first factor is the use of a thick air substrate ($\sim 0.13\lambda_0$), which has significantly reduced the total unloaded Q -factor of the CP patch cavity [23], thus widening the impedance bandwidth and AR bandwidth. The second one is the use of the probe-fed rectangular

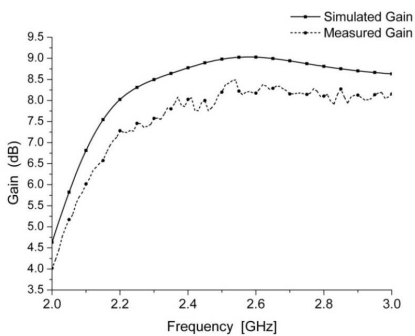


Figure 5. The simulated and measured maximum gain of this antenna.

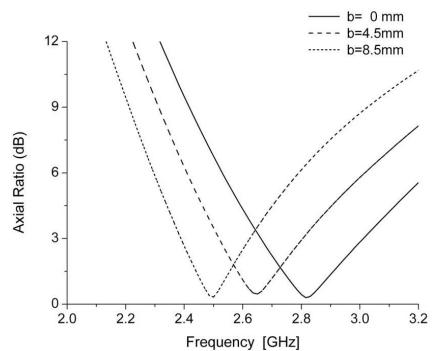


Figure 6. Simulated 3 dB AR versus frequency for different lengths of the two stubs.

strip, which functions as an impedance matching network that can broaden the impedance bandwidth and AR bandwidth further.

Figure 5 shows the simulated and measured maximum gain of this proposed CP antenna. The use of thick air-substrate and low-loss medium material (the dielectric loss tangent of the top substrate layer $\tan \delta = 0.0011$) in this design mainly leads to a maximum gain of 8.49 dBi at 2.54 GHz. Over the CP bandwidth (2.41~2.66 GHz), an average gain of about 8.16 dBi can be warranted. The discrepancy of the simulated and measured results can be considered as normal, which is mainly due to the power loss led by fabrication and the finite ground plane. In fabrication, a part of the fed power will be absorbed by the existed soldering tins in the practical antenna and the existed surface current on the finite metal ground plane will also consume some fed power. Both of the power loss can reduce the radiated power through the antenna thus bring down the gain of the antenna.

Figure 6 presents the simulated AR bandwidth versus frequency of the suspended corner truncated square patch antenna with different values of b , keeping all other parameters unchanged. It is obvious that the AR curve shifts toward lower frequency as b increases. When b equals 8.5 mm, the AR bandwidth well overlaps the impedance bandwidth at the center frequency. The variation can be explained by the fact that the two stubs, loaded at the non-radiating edges of the radiating patch, increase the overall effective resonant length of the radiating patch and thus reduce the resonant frequency of the CP antenna.

The radiation patterns of the proposed antenna in both E and

Table 1. Performance parameters of CP antennas on measurements.

Parameters	Corner truncated square patch with two stubs	E-shaped patch	H-shaped patch
Resonant Frequency	2.45 GHz	2.45 GHz	2.45 GHz
Impedance bandwidth (VSWR < 2.0)	770 MHz (31.43%)	260 MHz (10.27%)	490 MHz (19.4%)
3 dB AR bandwidth	250 MHz (10%)	400 MHz (16%)	560 MHz (22.5%)
Operating CP bandwidth	250 MHz (10%)	230 MHz (9.27%)	490 MHz (19.4%)
Gain	8.0 dBi	7.6 dBi	5.7 dBi

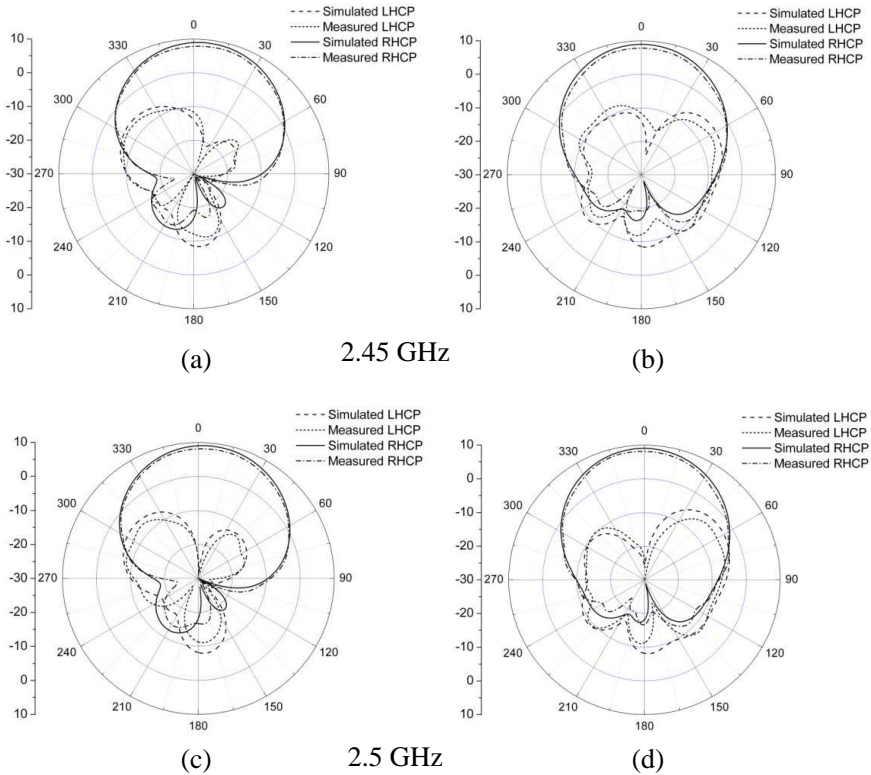


Figure 7. Simulated and Measured radiation patterns of the antenna of (a) (c) xoz -plane and (b) (d) yo z -plane.

H planes (yo z -plane and xoz -plane) are simulated and measured at 2.45 GHz, 2.5 GHz, as shown in Figure 7. It can be found that the measured results are well in accordance with the simulated results. Also the measured results show that the cross-polarization level (LHCP) is lower than the co-polarization level (RHCP) by more than 20 dB at the broadside direction, which is due to the fact that the probe-fed horizontal rectangular strip can provide the necessary capacitive reactance to compensate the inductive reactance caused by the vertical probes.

Since the broad-band circular-polarized stack antenna for 2.45 GHz systems is an interested research topic and useful in RFID and 802.11b/g WLAN band, a comparison of the proposed antenna in this paper with this kind of antennas in [18, 19] is made in Table 1. All of the three antennas are single-fed single-patch CP antennas. From

Table 1, we can see that the proposed antenna in this paper has a wider operating CP bandwidth and the highest gain in the three antennas, which make the antenna more suitable in practical application.

4. CONCLUSION

A novel probe-fed rectangular strip is proposed for feeding a single-patch microstrip patch antenna. The technique exhibits broadband, high-gain and low cross polarization characteristics. The designed antenna has an impedance bandwidth of 31.43% ($VSWR < 2$), a 3 dB axial ratio bandwidth of 10% and 22.45% for 6 dB axial ratio bandwidth, and an average gain of 8.16 dBi. The cross-polarization level (LHCP) is lower than the co-polarization level (RHCP) by more than 20 dB at the broadside direction. A parametric study of the two stubs is also presented. The two stubs with optimized lengths, loaded at the non-radiating edges of the radiating patch, can reduce the resonant frequency of the 3 dB AR effectively.

REFERENCES

1. Chang, T.-N. and J.-H. Jiang, "Enhance gain and bandwidth of circularly polarized microstrip patch antenna using gap-coupled method," *Progress In Electromagnetics Research*, Vol. 96, 127–139, 2009.
2. Heidari, A. A., M. Heyrani, and M. Nakhkash, "A dual-band circularly polarized stub loaded microstrip patch antenna for GPS applications," *Progress In Electromagnetics Research*, Vol. 92, 195–208, 2009.
3. Huang, Y.-H., S.-G. Zhou, J. Ma, and Q.-Z. Liu, "Optimization of three-dimensional (3-D) ground structure for improved circularly polarized microstrip antenna beamwidth," *Progress In Electromagnetics Research Letters*, Vol. 10, 135–143, 2009.
4. Sharma, S. B., D. A. Pujara, S. B. Chakrabarty, and V. K. Singh, "Removal of beam squinting effects in a circularly polarized offset parabolic reflector antenna using a matched feed," *Progress In Electromagnetics Research Letters*, Vol. 7, 105–114, 2009.
5. Chi, L.-P., S.-S. Bor, S.-M. Deng, C.-L. Tsai, P.-H. Juan, and K.-W. Liu, "A wideband wide-strip dipole antenna for circularly polarized wave operations," *Progress In Electromagnetics Research*, Vol. 100, 69–82, 2010.
6. Secmen, M. and A. Hizal, "A dual-polarized wide-band patch

- antenna for indoor mobile communication applications,” *Progress In Electromagnetics Research*, Vol. 100, 189–200, 2010.
7. Masa-Campos, J. L. and F. Gonzalez-Fernandez, “Dual linear/circular polarized planar antenna with low profile double-layer polarizer of 45° tilted metallic strips for WiMAX applications,” *Progress In Electromagnetics Research*, Vol. 98, 221–231, 2009.
 8. Chi, L.-P., S.-S. Bor, S.-M. Deng, C.-L. Tsai, P.-H. Juan, and K.-W. Liu, “A wideband wide-strip dipole antenna for circularly polarized wave operations,” *Progress In Electromagnetics Research*, Vol. 100, 69–82, 2010.
 9. Lee, J. M., N. S. Kim, and C. S. Pyo, “A circular polarized metallic patch antenna for RFID reader,” *Proceedings of Asia-Pacific Conference on Communications*, Perth, Western Australia, Oct. 2005.
 10. Wang, Z. B., S. I. Fang, and S. Q. Fu, “A low cost miniaturized CP antenna for UHF radio frequency identification reader applications,” *Microwave and Optical Technology Letters*, Vol. 51, Oct. 2009.
 11. Lo, W. K., J.-L. Hu, C. H. Chan, and K. M. Luk, “Circularly polarized patch antenna with an L-shaped probe fed by a microstrip line,” *Microwave and Optical Technology Letters*, Vol. 24, 412–414, 2000.
 12. Wang, C. and K. Chang, “Single-layer wideband probe-fed circularly polarized microstrip antenna,” *Proc. IEEE Antennas Propagat. Soc. Int. Symp. Dig.*, 1000–1003, Salt Lake City, UT, 2000.
 13. Karmakar, N. C. and M. E. Bialkowski, “Circularly polarized aperture-coupled circular microstrip patch antennas for L-band applications,” *IEEE Trans. Antennas Propag.*, Vol. 47, 933–940, May 1999.
 14. Lo, W. K., J. I. Hu, C. H. Chan, and K. M. Luk, “L-shaped probe-feed circularly polarized microstrip patch antenna with a cross slot,” *Microwave and Optical Technology Letters*, Vol. 25, No. 4, 251–251, May 2000.
 15. Chang, F. S., K. L. Wong, and T. Z. Chiou, “Low-cost broadband circularly polarized patch antenna,” *IEEE Trans. Antennas Propag.*, Vol. 51, Oct. 2003.
 16. Tong, K. F. and T. P. Wong, “Circularly polarized U-slot antenna,” *IEEE Trans. Antennas Propag.*, Vol. 55, No. 8, 2382–2385, Aug. 2007.

17. Yang, S. S., K.-F. Lee, A. A. Kishk, and K.-M. Luk, "Design and study of wideband single feed circularly polarized microstrip antennas," *Progress In Electromagnetics Research*, Vol. 80, 45–61, 2008.
18. Khidre, A., K. F. Lee, F. Yang, and A. Eisherbeni, "Wideband circularly polarized E-shaped patch antenna for wireless applications," *IEEE Trans. Antennas Propag.*, Vol. 52, No. 5, Oct. 2010.
19. Chung, K. L., "A wideband circularly polarized H-shaped patch antenna," *IEEE Trans. Antennas Propag.*, Vol. 58, No. 10, 3379–3383, Oct. 2010.
20. Sun, L., Y. H. Huang, J. Y. Li, and Q. Z. Liu, "A wideband circularly polarized candy-like patch antenna," *Journal of Electromagnetic Waves and Applications*, Vol. 25, Nos. 8–9, 1113–1121, 2011.
21. Wang, Z., S. Fang, S. Fu, and M. Fan, "Single-fed single-patch broadband circularly polarized antenna for UHF RFID reader applications," *2010 2nd International Conference on Industrial and Information Systems*, Vol. 1, 87–89, 2010.
22. Chen, Z. N. and M. Y. W. Chia, "Broad-band suspended probe-fed plate antenna with low cross-polarization levels," *IEEE Trans. Antennas Propag.*, Vol. 51, 345–346, 2003.
23. Lo, Y. T., D. Solomon, and W. F. Richards, "Theory and experiment on microstrip antennas," *IEEE Trans. Antennas Propag.*, Vol. 27, 137–145, Mar. 1979.